Available online at www.sciencedirect.com
SCIENCE DIRECT®
Mechanics of Materials 37 (2005) 275–285
MECHANICS OF MATERIALS
www.elsevier.com/locate/mechmat

Mechanics of hierarchical adhesion structures of geckos

Huajian Gao *, Xiang Wang [1], Haimin Yao, Stanislav Gorb, Eduard Arzt

Max Planck Institute for Metals Research, Heisenbergstrasse 3, D-70569 Stuttgart, Germany

Received 25 September 2003; received in revised form 1 February 2004

Abstract

Geckos (*Gekko gecko*) have evolved elaborate adhesive structures which allow them to move along vertical walls and ceilings against their body weight. There is strong evidence that the adhesion ability of geckos is due to the van der Waals interaction between a contacting surface and hundreds of thousands of keratinous hairs or setae on the gecko's foot; each seta is 30–130 μm long and contains hundreds of 200–500 nm projections or spatulae. While contact mechanics suggests that the refinement of structure size results in greater adhesive strength, some important questions remain unsolved: What is the significance of nanometer length scale for adhesion? What is the optimum adhesive strength of a structure? How can a structure optimized for attachment simultaneously allow easy detachment, as reversible adhesion is crucial for the animal's movement? In this paper, we show that the nanometer range of the spatula size of geckos may have evolved to optimize the adhesive strength and maximum tolerance of imperfect adhesion (for robustness). Our analysis also indicates that the asymmetrical structure of the gecko's seta structure may have been designed to simultaneously allow robust attachment and easy detachment.

Keywords: Adhesion; Contact mechanics; Biological materials; Nanostructured materials

1. Introduction

Geckos (*Gekko gecko*) and many insects possess extraordinary ability to move on vertical surfaces and ceilings. To these professional climbers, it is not difficult to wander, race, sprint and even fight on a smooth ceiling; rapid switches between attachment and detachment seem simple, easy and effective. Comparative studies of hundreds of insects and other animal species revealed that biological attachment systems basically converge to two principal designs: a "hairy" system consisting of finely structured protruding hairs with size ranging from a few hundred nanometers to a few microns, dependent upon the animal species, and a "smooth" system with relatively smooth surface covering a fine tissue microstructure (Scherge and

* Corresponding author. Tel.: +49 711 689 3510; fax: +49 711 689 3512.
E-mail address: hjgao@mf.mpg.de (H. Gao).
[1] Present address: Department of Engineering Mechanics, Tsinghua University, Beijing 100084, China.

0167-6636/$ - see front matter
doi:10.1016/j.mechmat.2004.03.008

Gorb, 2001; Niederegger et al., 2002; Gorb et al., 2000). Both systems are able to adapt to the profile of a contacting surface. Geckos, beetles, flies and spiders have adopted the hairy design. Experiments using freezing-substitution techniques and scanning electron microscopy have revealed many details of the ultrastructure of biological attachment pads. A gecko is found to have hundreds of thousands of keratinous hairs or setae on its foot; each seta is 30–130 μm long and contains hundreds of protruding submicron structures called spatulae (Fig. 1). Possible mechanisms of biological attachment include mechanical surface interlocking, fluid secretion (capillarity and viscosity) and molecular adhesion (van der Waals interaction). It is only recently that the development of MEMS techniques has allowed the adhesive force of geckos to be accurately measured at the level of a single seta (Autumn et al., 2000), with evidence that the dominant adhesion mechanism of geckos is the van der Waals interaction (Autumn et al., 2002).

If we consider the animal hairy systems, the density of setae strongly increases with the body weight of the animal, and geckos have the highest hair density among all animal species that have been studied (Scherge and Gorb, 2001). Various mechanical models have been developed to model specific hairy attachment systems, for instance the fiber arrays structure (Persson, 2003; Hui et al., 2002). In particular, the Johnson–Kendall–Roberts (JKR) model (Johnson et al., 1971) of contact mechanics has been used to show that splitting of a single contact into multiple smaller contacts always results in enhanced adhesion strength (Arzt et al., 2002, 2003; Autumn et al., 2002), thus providing a theoretical basis for understanding the hairy attachment system. One of the puzzling predictions of the JKR type model is that the spatula structure of geckos can be split ad infinitum to support arbitrarily large body weights. This is clearly impossible as the adhesion strength cannot exceed the theoretical strength of van der Waals interaction.

2. The JKR type contact mechanics model

To understand the apparent paradox caused by the JKR type model, consider a cylindrical spatula with a hemispherical tip with diameter $2R$ in contact with a smooth surface, as shown in Fig. 2a. The profile of the hemispherical tip can be described by a function $z = R - \sqrt{R^2 - r^2}$, where z

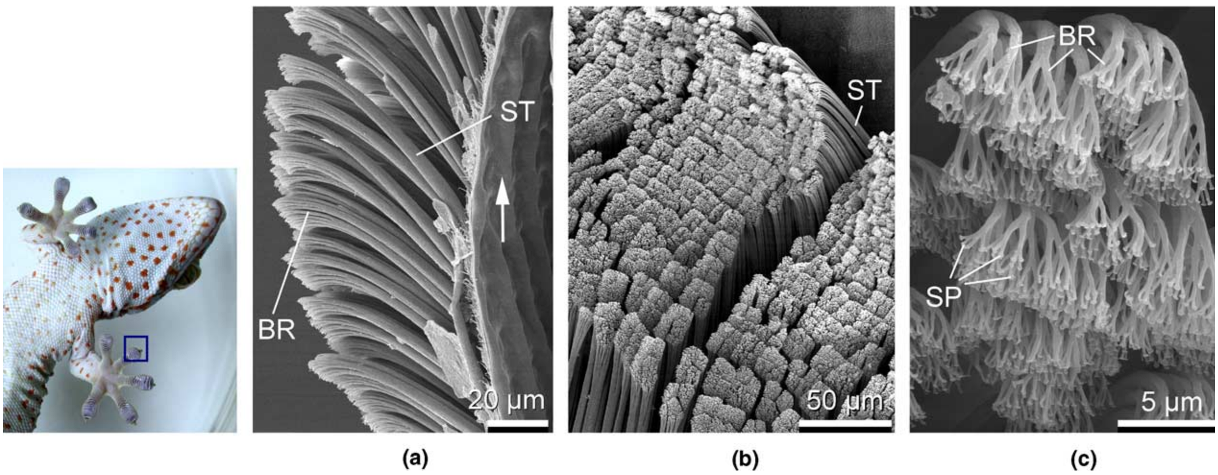

Fig. 1. The hierarchical adhesive structures of *Gekko gecko*. A toe of gecko contains hundreds of thousands of setae and each seta contains hundreds of spatulae. (a) and (b): scanning electron micrographs of rows of setae at different magnifications and (c): spatulae, the finest terminal branches of seta. ST: seta; SP: spatula; BR: branch.

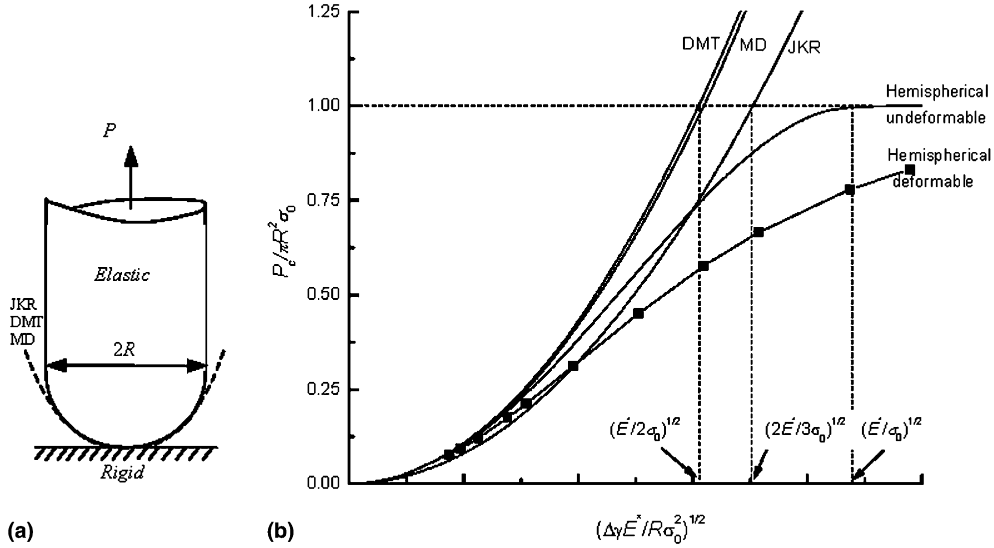

Fig. 2. Predictions of JKR type contact mechanics models for the adhesion strength of an elastic cylinder with a hemispherical tip on a rigid substrate: (a) geometry of a hemispherical tip and its parabolic approximation; (b) classical models of contact mechanics (JKR, MD, DMT) have adopted the parabolic approximation of the tip geometry and make incorrect predictions at very small sizes. The exact solutions for a hemispherical tip are labeled as "hemispherical undeformable" if elastic deformation of the tip is neglected and as "hemispherical deformable" if elastic deformation is taken into account. Unlike the JKR type models, the exact solutions show saturation at the theoretical strength of van der Waals interaction at very small sizes.

measures the height and r the planar radius of a point on the tip. The JKR model, as well as the Maugis–Dugdale (MD) model (Maugis, 1992) and the Derjaguin–Muller–Toporov (DMT) model (Derjaguin et al., 1975), are all based on the parabolic approximation $z = r^2/2R$ (dashed line in Fig. 2a) of the local geometry of the contacting body. Under the parabolic approximation, the JKR, MD and DMT models all predict unlimited increase in adhesive strength as the size of the contacting object is reduced (i.e., decreasing R), as shown in Fig. 2b. However, if the exact profile $z = R - \sqrt{R^2 - r^2}$, instead of the approximation $z = r^2/2R$, is used for the spatula tip, the adhesion strength will be capped by the theoretical strength of the van der Waals interaction σ_0. This can be most simply shown by the following calculations: First, consider a DMT type model in which the deformation of contacting objects is neglected and assume a simple Dugdale type interaction law (Dugdale, 1960) where the force is equal to σ_0 within a critical interacting distance $\Delta\gamma/\sigma_0$ and zero beyond this distance, $\Delta\gamma$ being the van der Waals interaction energy. The pull-off force, P_c, could be calculated as following (Bradley, 1932):

$$P_c = \int_0^R 2\pi r \sigma \, \mathrm{d}r. \tag{1}$$

The relation between the surface separation h and radius r is given by

$$h = R - \sqrt{R^2 - r^2}. \tag{2}$$

Therefore

$$(R - h)\, \mathrm{d}h = r\, \mathrm{d}r \quad \left(0 \leqslant h \leqslant \frac{\Delta\gamma}{\sigma_0}\right). \tag{3}$$

Substituting Eq. (3) into Eq. (1) and using the Dugdale interaction law, we immediately obtain

$$\frac{P_c}{\pi R^2 \sigma_0} = \begin{cases} 2\eta - \eta^2 & \eta < 1, \\ 1 & \eta \geqslant 1, \end{cases} \tag{4}$$

where $\eta = \Delta\gamma/(R\sigma_0)$. This result is plotted in Fig. 2b as the curve labeled "hemispherical undeformable". In contrast to the JKR model, there is clearly a saturation of adhesion strength below a critical size. When the radius of the spatula is smaller than $\Delta\gamma/\sigma_0$, the contact achieves its maximum strength, which is equal to the theoretical strength of the van der Waals interaction σ_0 (see Fig. 2b). The critical size for strength saturation $\Delta\gamma/\sigma_0$ is the effective range of the van der Waals interaction, which is typically on the order of a few atomic spacings. It is interesting to note that the classical models of JKR, DMT and MD in contact mechanics are unable to capture the process of strength saturation.

If elastic deformation is considered in the analysis of adhesive contact, an explicit expression for the pull-off force cannot be obtained. We have developed a numerical procedure to treat the case of a deformable hemispherical tip similar to the previous studies (Greenwood, 1997; Johnson and Greenwood, 1997), but with an important difference in that the hemispherical geometry is now exactly taken into account. Assuming a Lennard–Jones type interaction law between an elastic spatula and a rigid substrate (Greenwood, 1997), the pull-off force is calculated and plotted in Fig. 2b as the curve labeled "hemispherical deformable". It is seen that the pull-off force indeed asymptotically approaches the theoretical strength of the van der Waals interaction as the spatula size decreases.

The calculations with a hemispherical model of a spatula tip have confirmed that the maximum adhesive strength is the theoretical strength of the van der Waals interaction. However, for the hemispherical tip, the adhesive strength does not reach the maximum strength until the tip size falls below a few atomic spacings. This suggests that a hemispherical tip is a relatively poor design for adhesion. Indeed, broad studies of biological attachment devices (Scherge and Gorb, 2001) revealed that the spherical shape of contact elements is a very rare case in nature. Biological spherical contacts usually consist of an extremely compliant material (Spolenak et al., 2004).

What is the best shape of the spatula tip for optimizing adhesive strength? Here we only discuss the simplest case of a cylindrical spatula in frictionless contact with a rigid substrate, resembling a soft biological tissue in contact with a hard material. In this case, the best shape is simply a flat punch because there is no stress concentration for a flat punch in contact with a smooth rigid substrate if there are no defects over the contacting region; under such conditions the adhesive strength would be identical to the theoretical strength of the van der Waals interaction. In other words, a flat-ended spatula adhering to a flat rigid substrate would have the theoretical adhesion strength regardless of the size of contact. The only problem with such a design is that the strength would be highly sensitive to the existence of defects in the contact region. Slight variations in geometrical irregularities, impurities, contaminants, surface roughness, trapped air bubbles, and/or slightly skewed contact angles form crack-like defects and reduce the actual contact area, inducing stress concentration along the edge of the contact region and causing adhesion failure as the crack-like flaws spread.

3. Selection of nanometer size for robust adhesion

The most terminal structure of a gecko's attachment mechanism consists of the spatula (Fig. 1c) of a few hundred nanometers in diameter. Here we model the spatula as an elastic cylinder. Why is the spatula size in the nanometer range? To understand this, we model the spatula as an elastic cylinder with a flat tip. The radius of the cylinder is R. Imperfect contact between the spatula and substrate is assumed such that the radius of the actual contact area is $a=\alpha R$, $0<\alpha<1$, as shown in Fig. 3a; the outer rim $\alpha R<r<R$ represents flaws or regions of poor adhesion. The adhesive strength of such an adhesive joint can be calculated by treating the contact problem as a circumferentially cracked cylinder, in which case the stress field near the edge of the contact area has a square-root singularity with stress intensity factor (Tada et al., 2000)

$$K_I = \frac{P}{\pi a^2}\sqrt{\pi a}F_1(\alpha), \tag{5}$$

where $F_1(\alpha)$ varies in a narrow range between 0.4 and 0.5 for $0 \leqslant \alpha \leqslant 0.8$ ($\alpha=1$ corresponds to perfect, defect-free contact). Substitute Eq. (5) into the Griffith condition

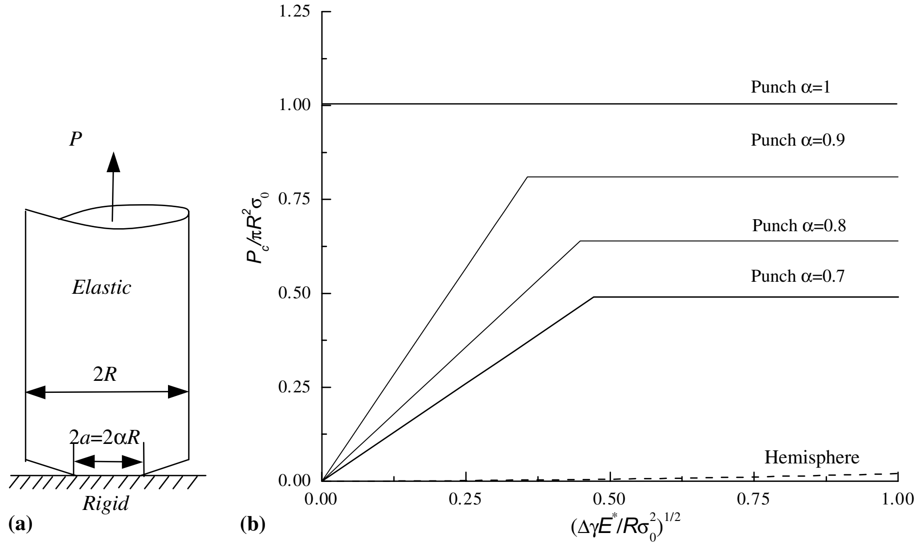

Fig. 3. Adhesion of a flat-ended cylinder to a rigid substrate. The actual contact area is assumed to be smaller than the total area of the punch due to imperfections along the outer rim of the punch. This contact model is elastically equivalent to a cracked cylinder. (a) Geometry of a flat punch partially adhering to a substrate. (b) Variations of the apparent adhesion strength for different actual contact areas according to Griffith criterion and theoretical strength. The JKR prediction of a hemispherical tip is plotted as a dashed line for comparison. The plot shows that a flat punch induces much larger adhesive forces in comparison with a hemispherical tip, and that the adhesion strength reaches the theoretical strength of van der Waals interaction at a critical contact size.

$$\frac{K_I^2}{2E^*} = \Delta\gamma, \tag{6}$$

where the factor 2 is due to the rigid substrate. The apparent adhesive strength normalized by the theoretical strength, $\hat{\sigma}_c = P_c/\sigma_0\pi R^2$, is obtained as

$$\hat{\sigma}_c = \beta\alpha^2\psi, \tag{7}$$

where

$$\psi = \sqrt{\frac{\Delta\gamma E^*}{R\sigma_0^2}}, \tag{8}$$

$$\beta = \sqrt{2/\pi\alpha F_1^2}, \quad E^* = E/(1-\nu^2), \tag{9}$$

E and ν being the Young's modulus and Poisson's ratio, respectively. The adhesive strength is a linear function of the dimensionless variable ψ with slope $\beta\alpha^2$. The maximum adhesion strength is achieved when the pull-off force reaches $P_c = \sigma_0\pi a^2$, or $\hat{\sigma}_c = \alpha^2$, in which case the traction within the contact area uniformly reaches the theoretical strength σ_0. This saturation in strength occurs at a critical size of the contact area

$$R_{\rm cr} = \beta^2 \frac{\Delta\gamma E^*}{\sigma_0^2}. \tag{10}$$

Fig. 3b plots the apparent adhesive strength for $\alpha = 0.7$, 0.8 and 0.9, together with the case of flawless contact ($\alpha = 1$). The corresponding result of a hemispherical tip based on the JKR model is plotted as a dashed line for comparison. Clearly, the flat-ended spatula achieves the maximum adhesion strength much more "quickly" than the hemispherical configuration.

The critical contact size for saturation of adhesion strength can be estimated as follows. Assume the actual contact area is about 50% of the total area available for contact, corresponding to $\alpha \cong 0.7$. The parameters for the van der Waals interaction and the Young's modulus of the spatula (keratin) are selected as follows:

$$\sigma_0 = 20\ \text{MPa}, \quad \Delta\gamma = 0.01\ \text{J/m}^2,$$
$$\frac{\Delta\gamma}{\sigma_0} \cong 0.5\ \text{nm}, \quad E^* = 2\ \text{GPa}. \tag{11}$$

This gives the critical size for strength saturation as

$$R_{cr} \cong 225 \text{ nm}. \tag{12}$$

Interestingly, the radius of the gecko's spatula is typically around 100–250 nm. The above analysis suggests that the nanometer size of the spatula structure of geckos may have evolved to achieve optimization of adhesive strength in tolerance of possible contact flaws.

Below the critical size R_{cr}, it can be expected that the adhesion traction within the contact region is maintained uniformly at the theoretical strength, indicating that the stress concentration near the edge of the contact area should vanish for sufficiently small contact. To illustrate this point, we have analyzed in some detail the elastic punch model with $\alpha = 0.7$ using a cohesive surface model developed by Tvergaard and Hutchinson (1996) implemented in a finite element code (Klein et al., 2001).[2] Other cohesive models (Barenblatt, 1959; Willis, 1967; Rose et al., 1981; Xu and Needleman, 1994; Rahulkumar et al., 2000) could in principle also be used to model molecular adhesion. The Tvergaard–Hutchinson model is selected because it preserves the van der Waals energy regardless of the peeling orientation. Other cohesive models with various considerations of tension versus shear dominated separation do not necessarily preserve the interaction energy. The computational results of the pull-off force plotted in Fig. 4a clearly indicate saturation in the adhesion strength as the critical contact size is approached.

Fig. 4b shows the traction distribution within the contact region at the critical pull-off force for four different spatula sizes, corresponding to the four data points in Fig. 4a. It is observed that the traction becomes more uniform with decreasing structure size. Below the critical size, the stress concentration near the edge of the contact area completely vanishes and the adhesive structure maintains a state of uniform contact force despite of the crack-like flaw around the outer edge.

The selection of nanometer size for robust design of materials has already been discussed in our previous study (Gao et al., 2003; Gao and Yao, 2004) of fracture strength optimization in the nanocomposite structure of biological materials. The present study of adhesion strength in biological attachment structures again highlights the prevalence of flaw-tolerant design in biology.

[2] The computation is performed based on the code developed by Dr. Patrick Klein of Sandia National Laboratory (http://tahoe.ca.sandia.gov).

4. Anti-bunching condition of the spatula structure

The van der Waals interaction may cause clustering or bundling of adjacent spatulae due to their relatively large aspect ratios. Stability of spatulae against bundling is a necessary condition for their viability as an adhesion structure. Recent study (Geim et al., 2003) has demonstrated that bunching leads to reduction of adhesive strength in the microfabricated artificial gecko structure made of polyimide micro-hairs. To gain some insight into this issue, we model the spatula as a cantilever beam with square cross section. The configuration of a pair of adjacent spatulae in the free-standing state is shown in Fig. 5a, and that in the state of clustering is shown in Fig. 5b. Stability against bunching is interpreted as that the bundled state of Fig. 5b should be unstable and will spontaneously detach if formed. This problem can be treated as a crack problem with detachment condition (Hui et al., 2002; Tada et al., 2000)

$$E^* \geqslant \frac{8\gamma l^4}{3\Delta^2 t^3}, \tag{13}$$

where γ is the surface energy per unit area of each surface and the geometrical parameters l, Δ, t are shown in Fig. 5a. A different condition of bunching instability has been derived by Persson (2003) who compared the energy of fibers bent over a curvature to that of straight fibers. In contrast, there is no need to consider a bent fiber structure in our analysis. As a rough estimate we may choose (e.g., Autumn et al., 2000, 2002)

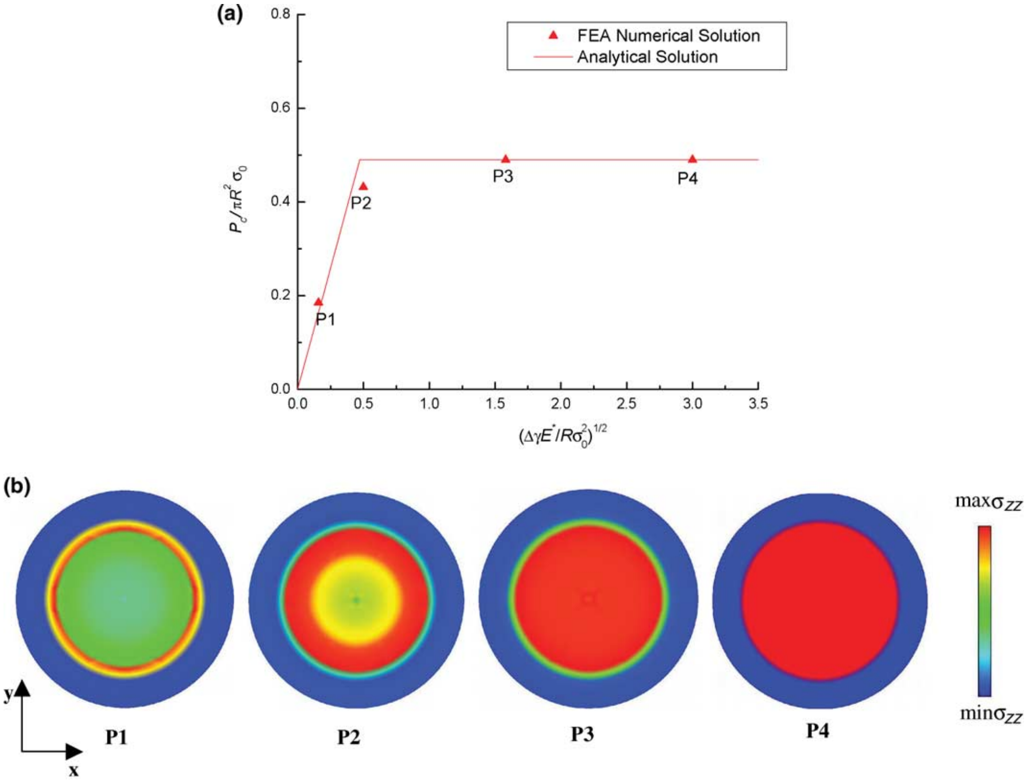

Fig. 4. Numerical results of the Tvergaard–Hutchinson model for the adhesion of a flat-ended cylinder partially adhering to a rigid substrate. The real contact area is assumed to be 50% of the total area of the punch ($\alpha = 0.7$). (a) The normalized pull-off force shows saturation at a critical size, in good agreement with the simple analysis from Griffith criterion. (b) The traction distribution within the contact area becomes more uniform as the size is reduced. Below the critical size, the traction becomes uniform and equal to the theoretical strength of van der Waals interaction. An arbitrary scale has been used here to plot the traction distribution.

$$\Delta = 0.6\ \mu\text{m}, \quad t = 0.2\ \mu\text{m},$$
$$l = 2\ \mu\text{m}, \gamma = 0.01\ \text{J/m}^2. \tag{14}$$

The stability condition (13) suggests a minimum Young's modulus of 0.15 GPa. Biological materials such as keratin have Young's modulus on the order of a few GPa and thus meet the stability condition. For a hemispherical tip, the critical size to achieve theoretical strength is on the order of $t = 1$ nm. At this length scale, the stability condition requires a minimum Young's modulus on the order of 10^5 GPa, which is impossible to meet. The advantage of the flat punch design of the spatula over the hemispherical design is thus two-fold. The flat punch design not only allows the system to maximize adhesive strength more efficiently, but it is also required from the point of view of structural stability.

5. Hierarchical design for reversible adhesion: the asymmetrical structure of a seta

A unique feature of biological attachment systems is that the adhesion must be easily overcome to allow rapid switches between attachment and detachment during the animal's motion. It seems that geckos achieve such reversibility via a unique design of their seta structure, which is one hierarchy above the spatula structure. A seta contains hundreds of spatulae and has characteristic sizes on the order of tens of microns. While spatulae

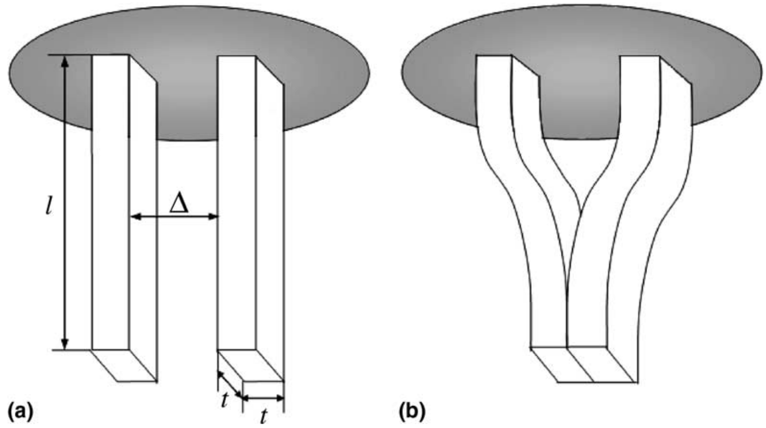

Fig. 5. Stability of two adjacent elastic protrusions (spatulae) against self-bundling. Configurations of two (a) free standing and (b) self-bundled protrusions. The stability of the structure is defined such that the bundled configuration would spontaneously separate into the free standing configuration.

provide adhesion strength, hundreds of thousands of setae act together to provide the total attachment force to support the gecko's body weight. At the level of a single seta, spatulae could be modeled as a cohesive layer over the tip surface of the seta. We have constructed a finite element model of a single seta, as shown in Fig. 6. A layer of a cohesive element is inserted between the contacting surface at the tip of the seta and the rigid substrate. The cohesive energy of the adhesive layer (spatula) includes not only the van der Waals energy but also the elasticity of the spatula. This en-

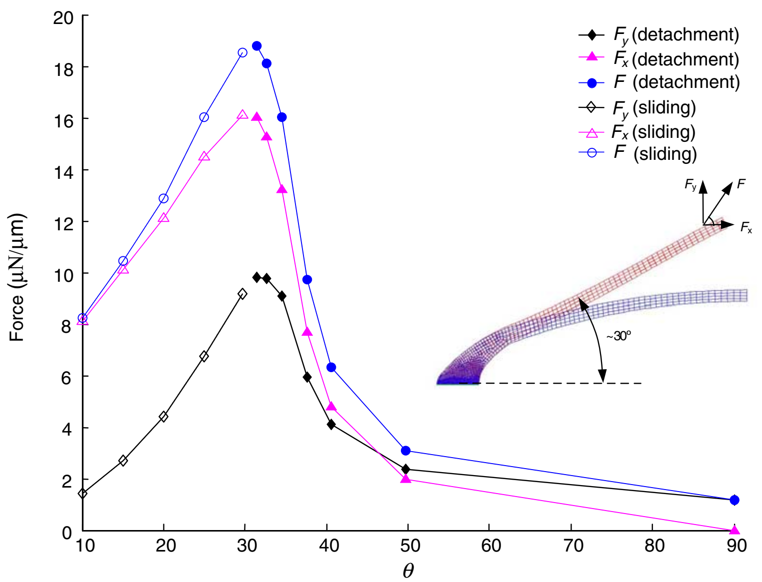

Fig. 6. Analysis of the pull-off force of a single seta as a function of the pulling orientation. The plot shows that the asymmetrical structure of the seta causes more than an order of magnitude change in adhesive force as the pulling angle varies between 30° and 90°. This allows for the possibility of fast switch between attachment and detachment.

ergy is estimated to be around 0.4 J/m^2, about an order of magnitude higher than the van der Waals energy ($\Delta\gamma = 0.01$–0.05 J/m^2). Material properties of setae are selected as $E = 1$ GPa, $\nu = 0.3$. A pulling force at an angle θ with respect to the contact surface is exerted at the other end of the seta to simulate the muscular action of the animal.

The computational results (Fig. 6) show that there exist two mechanisms of adhesive failure, detachment from or sliding with respect to the substrate, dependent upon the pulling angle θ. For θ smaller than 30°, sliding occurs before detachment, whereas for θ larger than 30°, detachment becomes the dominant mechanism of adhesion failure. Maximum attachment force is achieved when force is exerted at around a 30° angle. Interestingly, both the parallel and perpendicular components of the detachment force reach their maximum at the 30° orientation. These force components play a crucial role when a gecko moves along vertical walls or ceilings. The analysis suggests that the gecko would apply muscular force to pull at a 30° angle in order to maximize the adhesive force when strong attachment is desired. The pull-off force at 90° (the peeling mode) is an order of magnitude smaller than the maximum attachment force at 30°, suggesting that the gecko would use peeling for detachment. This is consistent with the observation of gecko motion (Russell, 1975). Therefore, it appears that the asymmetrically designed seta structure is particularly suitable for rapid switching between attachment (30° pulling) and detachment (90° peeling).

The reason that the adhesion force at the pulling direction of 30° is much larger than that at 90° is due to the particular design of the seta which allows the most vulnerable point of failure initiation near the inner edge of contact to be "locked" (30°) and "unlocked" (90°). When the pulling force is applied at 30°, there is a net moment in the clockwise direction. This moment causes a local compressive stress near the inner edge of contact, effectively "locking" this site for crack initiation. When the force is applied above 30° and approaches the peeling mode, the resultant moment becomes counter-clockwise and helps "unlocking" the inner edge of contact as a crack initiation site for easy detachment. This design allows the gecko to switch between attachment and detachment simply by controlling the action of different muscles. In addition to skeletal muscles common to most animal species, the gecko has evolved special muscles and joint design allowing so-called digital hyperextension, which is essential for the peeling action required for detachment (Russell, 1975), as shown in Fig. 7.

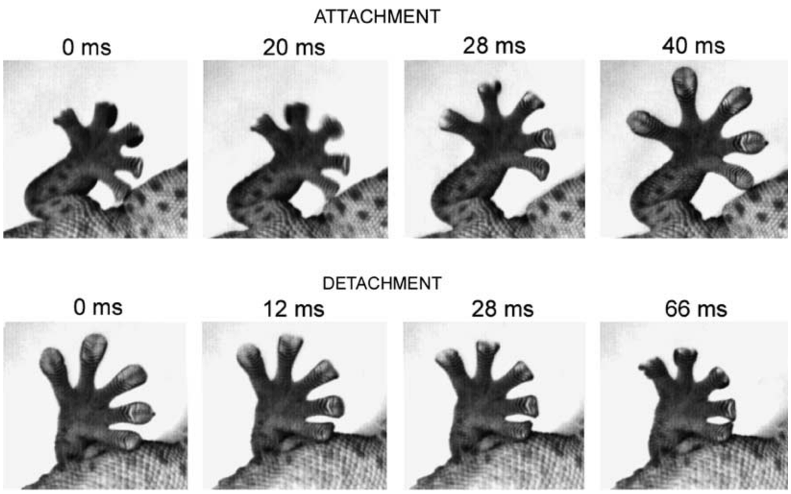

Fig. 7. Snapshots of gecko attachment and detachment from a glass ceiling. Peeling is used to achieve detachment via special muscles and joint design allowing so-called digital hyperextension.

6. Summary and outlook

In this paper, we presented an example of how nature designs hierarchical structures to achieve robust and reversible attachment in the adhesion structures of geckos. We have shown that the nanometer size of the spatula, the most terminal adhesive structure of geckos, may have evolved to achieve maximum adhesion strength and at the same time tolerate potential contact flaws. The tolerance of flaws is the key to robust design and robustness is the key to survival. A similar concept has been previously developed (Gao et al., 2003) for the nanocomposite structure of biological materials. Here we have also shown that the limited range of materials choice (keratinous proteins) makes it even more necessary to evolve optimum structures to maximize adhesion and at the same time ensure structural stability. On the higher level of hierarchy, the asymmetrical structural design of setae may have evolved to achieve reversible adhesion allowing for easy and quick switches between attachment and detachment essential for locomotion. We hope that this study would serve as a small example of how mechanics can explain the principles of biological design.

In the 21st century, mechanics as a field will face many new challenges, one of which will be to assist materials scientists and engineers to develop novel hierarchical materials by nanoscale engineering. The development of nanotechnology promises to eventually enable us to design materials using a bottom-up approach, i.e., by constructing complex functional material systems by tailor-designing structures from atoms up. In this concerted venture of far-reaching significance to humanity, mechanics will have to revive itself and play a leadership role in developing fundamental theories of nanomaterials engineering. Currently, we barely have any theoretical basis on how to design a hierarchical material system to achieve a particular function. Nature can play the role of teacher, at least in the beginning stage, and mechanics will lead the way.

Acknowledgments

Support of this work has been provided by the Max Planck Society, the National Science Foundation of China and the Chang Jiang Scholar program through Tsinghua University. Discussions with Dr. Keller Autumn and Dr. Ralph Spolenak are gratefully acknowledged.

References

Arzt, E., Enders, S., Gorb, S., 2002. Towards a micromechanical understanding of biological surface devices. Z. Metallk. 93, 345–351.

Arzt, E., Gorb, S., Spolenak, R., 2003. From micro to nanocontacts in biological attachment devices. Proc. Natl. Acad. Sci. USA 100, 10603–10606.

Autumn, K., Liang, Y.A., Hsieh, S.T., Zesch, W., Wai, P.C., Kenny, T.W., Fearing, R., Full, R.J., 2000. Adhesive force of a single gecko foot-hair. Nature 405, 681–685.

Autumn, K., Sitti, M., Liang, Y.A., Peattie, A.M., Hansen, S., Sponberg, S., Kenny, T.W., Fearing, R., Israelachvili, R.J., Full, R.J., 2002. Evidence for van der Walls adhesion in gecko setae. Proc. Natl. Acad. Sci. USA 99, 12252–12256.

Barenblatt, G.I., 1959. The formation of equilibrium cracks during brittle fracture. General ideas and hypotheses. Axially-symmetric cracks. Appl. Math. Mech. (PMM) 23, 622–636.

Bradley, R.S., 1932. The cohesive force between solid surfaces and the surface energy of solids. Phil. Mag. 13, 853–862.

Dugdale, D.S., 1960. Yielding of steel sheets containing slits. J. Mech. Phys. Solids 8, 100–104.

Derjaguin, B.V., Muller, V.M., Toporov, Y.P., 1975. Effect of contact deformations on the adhesion of particles. J. Colloid Interface Sci. 53, 314–326.

Gao, H., Ji, B., Jaeger, I.L., Arzt, E., Fratzl, P., 2003. Materials become insensitive to flaws at nanoscale: lessons from nature. Proc. Natl. Acad. Sci. USA 100, 5597–5600.

Gao, H., Yao, H., 2004. Shape insensitive optimal adhesion of nanoscale fibrillar structure. Proc. Natl. Acad. Sci. USA 101, 7851–7856.

Geim, A.K., Dubonos, S.V., Grigorieva, I.V., Novoselov, K.S., Zhukov, A.A., Shapoval, S.Yu., 2003. Microfabricated adhesive mimicking gecko foot-hair. Nature Mater. 2, 461–463.

Gorb, S., Jiao, Y., Scherge, M., 2000. Ultrastructural architecture and mechanical properties of attachment pads in *Tettigonia viridissima* (Orthoptera, Tettigoniidae). J. Comp. Physiol. A 186, 821–831.

Greenwood, J.A., 1997. Adhesion of elastic spheres. Proc. R. Soc. Lond. A 453, 1277–1297.

Hui, C.Y., Jagota, A., Lin, Y.Y., Kramer, E.J., 2002. Constraints on microcontact printing imposed by stamp deformation. Langmuir 18, 1394–1407.

Johnson, K.L., Greenwood, J.A., 1997. An adhesion map for the contact of elastic spheres. J. Colloid Interface Sci. 192, 326–333.

Johnson, K.L., Kendall, K., Roberts, A.D., 1971. Surface energy and the contact of elastic solids. Proc. R. Soc. Lond. A 324, 301–313.

Klein, P.A., Foulk, J.W., Chen, E.P., Wimmer, S.A., Gao, H., 2001. Physics-based modeling of brittle fracture: cohesive formulations and the application of meshfree methods. Theor. Appl. Fracture Mech. 37, 99–166.

Maugis, D., 1992. Adhesion of spheres: the JKR–DMT transition using a Dugdale model. J. Colloid Interface Sci. 150, 243–269.

Niederegger, S., Gorb, S., Jiao, Y., 2002. Contact behaviour of tenent setae in attachment pads of the blowfly *Calliphora vicina* (Diptera, Calliphoridae). J. Comp. Physiol. A 187, 961–970.

Persson, B.N.J., 2003. On the mechanism of adhesion in biological systems. J. Chem. Phys. 118, 7614–7621.

Rahulkumar, P., Jagota, A., Bennison, S.J., Saigal, S., 2000. Cohesive element modeling of viscoelastic fracture: application to peel testing of polymers. Int. J. Solids Struct. 37, 1873–1897.

Rose, J.H., Ferrante, J., Smith, J.R., 1981. Universal binding energy curves for metals and bimetallic interfaces. Phys. Rev. Lett. 47, 675–678.

Russell, A.P., 1975. A contribution to the functional analysis of the foot of the Tokay, *Gekko gecko* (Reptilia, Gekkonidae). J. Zool. Lond. 176, 437–476.

Scherge, M., Gorb, S., 2001. Biological Micro and Nano-Tribology. Springer-Verlag, New York.

Spolenak, R., Gorb, S., Gao, H., Arzt, E., 2004. Effects of contact shape on biological attachments. Proc. R. Soc. Lond. A, in press.

Tada, H., Paris, P.C., Irwin, G.R., 2000. The Stress Analysis of Cracks Handbook. ASME Press, New York.

Tvergaard, V., Hutchinson, J.W., 1996. Effect of strain-dependent cohesive zone model on predictions of crack growth resistance. Int. J. Solids Struct. 33, 3297–3308.

Willis, J.R., 1967. A comparison of the fracture criteria of Griffith and Barenblatt. J. Mech. Phys. Solids 15, 151–162.

Xu, X.P., Needleman, A., 1994. Numerical simulations of fast crack growth in brittle solids. J. Mech. Phys. Solids 42, 1397–1434.